ORIGINAL PAPER

Application of Metastructures for Targeted Low-Frequency Vibration Suppression in Plates

Ratiba F. Ghachi[1] · **Ahmed S. Mohamed**[2] · **Jamil Renno**[2] · **Wael Alnahhal**[1]

Abstract

Purpose We present an approach that combines finite element analysis and genetic algorithms to find the optimal configuration of local resonators created in the host structure to suppress their vibration in a target low-frequency range. Such local resonators are indeed metastructures that alter the wave propagation in the host structure, thereby attenuating their vibration.
Methods To demonstrate the approach, we cutout zigzag resonators in a thin aluminium plate that is subjected to base-excitations. The thin plate and the zigzag cutouts are modelled using the finite element method, and the optimal location and optimal tip mass of the zigzag cutouts are obtained using genetic algorithms through iterative simulations. Two case studies are considered, and the fitness function used in the optimization problem is the plate's root mean square of vibration in a specific low-frequency range. In the first case, the plate has two aligned zigzag cutouts. In this case, the objective is to find the optimal linear location and tip masses of the two zigzag cutouts. In the second case, the plate also has two zigzag cutouts, but their linear and transverse locations can vary along with the respective tip masses. The two optimal specimens are manufactured and tested experimentally.
Results Numerical results were compared to experimental results which demonstrate that the proposed approach is reliable and can be used to tune the band gap of plates, thereby maximizing the vibration attenuation in the target frequency range.
Conclusion Genetic algorithms can be used along with finite element analysis and zigzag cutouts to tune the band gap of plates subjected to base-excitations. The approach can be extended to plates/structures with other types of excitations and boundary conditions.

Keywords 2D metastructure · Multiobjective optimization · Genetic algorithm · Finite element simulation · Vibration attenuation

Introduction

The demand for thin and lightweight structural components is driven by customer and regulatory requirements for optimal mechanical designs. However, such structural components are usually flexible and lightly damped, requiring the design and implementation of vibration suppression techniques to ensure adequate in-service performance. Active,

Ratiba F. Ghachi and Ahmed S. Mohamed have contributed equally.

✉ Jamil Renno
jamil.renno@qu.edu.qa

1 Department of Civil and Architectural Engineering, Qatar University, PO Box 2713, Doha, Qatar

2 Department of Mechanical and Industrial Engineering, Qatar University, PO Box 2713, Doha, Qatar

semi-active, and passive vibration suppression techniques have been proposed to address this design requirement. Among passive vibration techniques that have been proposed by researchers and gained much attention recently is the use of metamaterials and metastructures. Inserting metamaterials or creating metastructures can alter wave propagation patterns in the host structure, thereby reducing its vibration. For example, the Bragg scattering effect in one-dimensional (1D) [1, 2], two-dimensional (2D) [3, 4], and three-dimensional (3D) [5, 6] metamaterials lead to the occurrence of frequency band gaps in periodically changing materials which contribute to vibration suppression. However, the center of the lowest frequency gap in such applications is about twice the lattice constant [7]. Thus, the sample's material and structural configuration affect the occurrence of the low transmission zone. An alternative approach to passive vibration suppression is using local resonant substructures;

this approach was first proposed by Liu et al. [8]. Locally resonant materials or substructures may comprise a matrix of scatterers that resonate and interact with the host structure's long wavelengths, thus restricting the propagation of the waves through the host structure. Pai [9] showed that the idealized models of uniform isotropic bars or tiny spring-mass subsystems could be used only for elastic waves having wavelengths much longer than the unit cell's length. Sun et al. [10] also showed that to absorb low-frequency waves, boundary conditions and resonant modes of the structure need to be considered at the design stage [10]. Thus, the local resonance's long-wavelength, low-frequency zones depend on their natural frequency and substructure design. Different resonant materials have been proposed to achieve this effect.

Single degree of freedom (SDOF) oscillators have also been used to suppress vibration. The inclusion of vibration dissipating components in a host structure permits the reduction of vibration transmission within the desired frequency range while ensuring the continued performance of the host structure's original function. In this approach, the SDOF oscillator is designed so that its natural frequency is very close to the frequency at which the host structure's vibration is to be reduced. Many researchers used SDOF oscillators for attenuating vibration in beams [11–15]. These studies have shown that SDOF oscillators contribute to vibration attenuation and that the low transmission zone depends on the resonance frequency of the inserted oscillator. However, the contribution of SDOF oscillators to suppressing the vibration of the host structure is usually limited to a narrow frequency band around their natural frequency. Recently, researchers proposed using zigzag beams as local resonators in host structures (often beams) that can be used instead of more traditional SDOF oscillators. In this regard, Hobeck and Inman [16] demonstrated experimentally that a cantilevered zigzag beam with low natural frequency can generate a low transmission zone to reduce vibration in the host structure. Essink and al. [17] and Karami and Inman [18] proposed structures with zigzag inserts for piezoelectric energy harvesting. Abdeldjaber et al. [19] proposed a closed-form approach to optimizing zigzag inserts for vibration attenuation. Numerical work on modeling the zigzag inserts assumes that the zigzag inserts are cantilevered to the host structure with no further interaction with the host structure. Chen et al. [14] used a zigzag configuration on the walls of a hollow square cross-section bar. They argued that the zigzag topology allows realizing a lower stiffness within a confined space. Despite the work done in this area, there is a lack of experimental results studying the geometric non-linearity of zigzag metastructures [20, 21] and focusing on vibration attenuation with minimum intervention on the host structure. Furthermore, the optimization of zigzag inserts has not been studied in the literature.

This paper proposes using finite element analysis to model a structure with zigzag cutouts. The finite element model is coupled with a genetic algorithm (GA) to find the optimal location and tip mass of the zigzag cut-outs. The zigzags will not be inserted into the structure but will rather be cut out using a laser cutting machine. The objective of the optimization is to find the optimal location of the cut-outs and the optimal mass to be placed at the tip of the zigzag to attenuate the structure's vibration in a specific frequency range and consequently transform the resonance frequency band around the plate's natural frequency to a low transmission zone. Previous researchers only used local resonators to suppress the vibration of the host structure at a specific frequency; however, in this paper, the fitness function of the GA is the root-mean-square of the vibration of the host structure at a specific location and in a target frequency range. Thus, identifying the "best location" for placing the zigzag cutouts becomes less obvious, and the use of the GA for the optimization process becomes evident. Although the presented approach is demonstrated numerically and experimentally on two plate structures with zigzag cutouts, the approach can be extended to further structures and other cutouts. Thus, this paper fills a gap in the literature and presents an approach that can be applied to minimize the vibration of a host structure with other cutouts.

Experimental Setup

Experiments were performed on thin aluminum plates with cut-out zigzags (Fig. 1), manufactured using a laser cutting machine, and a tip mass can be placed at the free end of the zigzag. The plates are clamped to a horizontal shaker (Fig. 2), exciting the plate at its base in the direction perpendicular to its plane. An APS 400 exciter is used due to its suitability for low-frequency investigations. The entire test setup is placed on a passive optical table (Model T46H-PTP602, Thorlabs) to ensure isolation from ambient vibrations. Two accelerometers were used to record the input and output signals, namely a miniature accelerometer (Type 4394 piezoelectric CCLD accelerometer, Brüel & Kjær) and a Piezoelectric Accelerometer, TEDS (Type 8344, Brüel & Kjær), respectively. The input and output accelerometers were placed at the vertical midline of the plate, at points i and j, respectively (Fig. 3). A swept sine signal ranging from 1 to 100 Hz is introduced at the base of the plate, and the frequency response function (FRF) is determined from the Fourier transform ratio of the output and the input acceleration signals. A schematic of the experimental setup is shown in Fig. 2.

Two types of aluminum plates were considered for optimization, P1 and P2. Details of plates P1 and P2 geometries are found in Table 1. Two control plates, R1 and R2, with
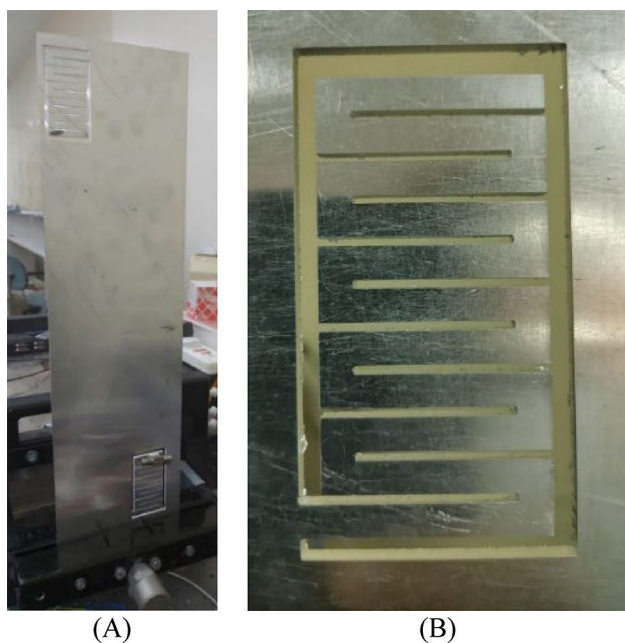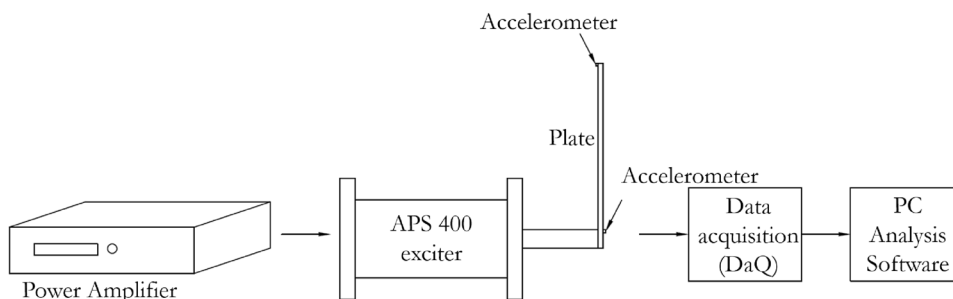
Fig. 1 Plate with zigzag cutouts: **A** plate with two zigzags and **B** close-up of the zigzag

randomly placed zigzags and tip masses (Table 1), are tested along with P1 and P2 for vibration transmission. The plates are clamped at 40 mm, resulting in a free height of 460 mm. The tested specimens are shown in Fig. 4, and the zigzag dimensions are detailed in Table 2 and Fig. 5.

The frequency response functions (FRFs) of the specimens P1, R1, P2, and R2 are plotted in Fig. 6. Figure 6A shows that the first two flexural modes of P1 are around 10 and 67 Hz. Plate R1 is obtained by cutting out two zigzags (at random locations) in P1 and adding random tip masses to the free ends of the zigzags. The first two flexural modes of R1 are around 6.5 and 64 Hz, depicted in Fig. 6A, which are slightly lower than their corresponding counterparts in P1 due to the reduction in mass and stiffness resulting from cutting out material to construct the zigzags. Around 48 and 57 Hz, two peaks emerged in R1 (Fig. 6A); these peaks correspond to the two randomly located zigzag cutouts forming a low transmission zone around 52 Hz. In Fig. 6B, the first

two flexural modes of P2 are around 10 and 69 Hz. Plate R2 is obtained by cutting out two zigzags (at random locations) in P2 and adding tip masses to the free ends of the zigzags. The first flexural mode of R2 is about 6.5 Hz (Fig. 6B), as its corresponding counterpart in P2, due to the plate's large size compared to the zigzags. Two peaks around 43 and 72 Hz emerged in R2 (Fig. 6B); these peaks correspond to the two randomly located zigzag cutouts, forming two narrow, low transmission zones around 43 and 72 Hz. Adding two zigzag cutouts with masses allows for minimum intervention to the host structure; however, obtaining a low transmission frequency zone using two zigzags requires optimizing the zigzags' position and tip masses. Experimental results of the two random plates with zigzags show that two zigzag cutouts can develop low transmission zones in the low-frequency zone without significantly affecting the stiffness and mass of the plate.

Optimization Process

In this section, we will use the experimental results presented in the previous section to optimize the location and the tip mass of the zigzag cutouts in plates P1 and P2 (Fig. 4). The optimization algorithm we will use is the genetic algorithm

Fig. 3 Aluminum plates with zigzag cutouts, accelerometers are placed at the input location (i) and at the output location (j). The structure is clamped to the shaker at location (i) and free at location (j)

Fig. 2 Schematic of the experimental setup. The entire setup is placed on an optical table (Model T46H-PTP602, Thorlabs) to isolate the experiment from ambient vibration
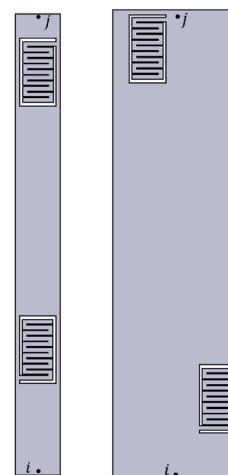
Table 1 Testing matrix: all plates have a thickness of 3 mm

Specimen name	Plate size $H \times W \times T$ (in mm)	Zigzag cutout location (mm)		Tip masses (g)
		Zigzag 1 (x,y)	Zigzag 2 (x,y)	
Plain (P1)	500×49×3	–		–
Random (R1)	500×49×3	(5, 99.1)	(5, 400)	4.71, 5.77
Plain (P2)	500×135×3	–		–
Random (R2)	500×135×3	(91.9, 49.3)	(17.3, 422.1)	14.9, 1.2

Fig. 4 Plate specimens: two control plates (P1 and P2) and two plates with zigzag cutouts at random locations and random masses at their free ends (R1 and R2)

(P1)   (R1)   (P2)   (R2)
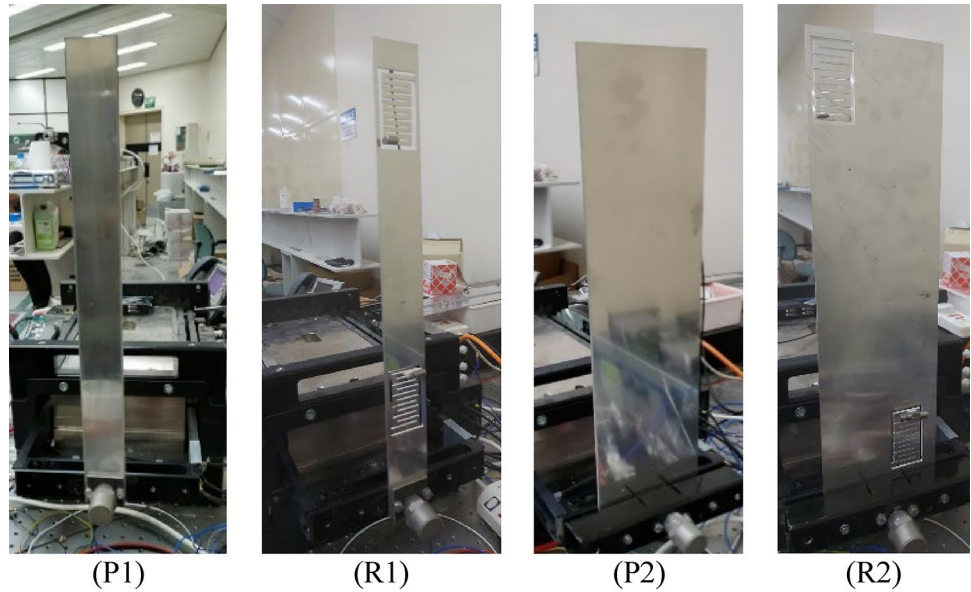
Table 2 Zigzag dimensions—see Fig. 5 for the schematic of the zigzag

Zigzag parameters	Values
α-beam length	28 mm
α-beam width	5 mm
β-beam length	6.1 mm
β-beam width	5 mm
Number of α-beams	11

Fig. 5 Description of the zigzag geometry
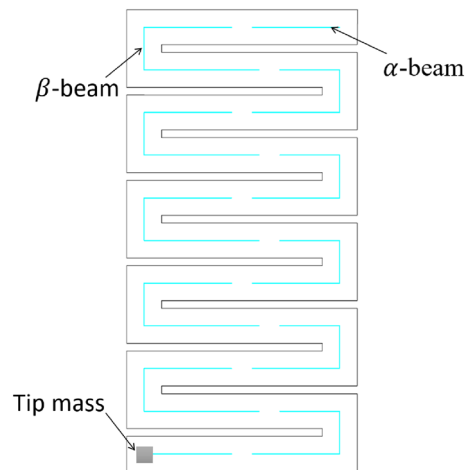
(GA) which will be used in conjunction with a finite element model of P1 and P2. The approach is detailed below.

Optimization Parameters

As demonstrated in Fig. 6A, B, the zigzag cutouts introduce a resonance in the range (60–80 Hz). Thus, we propose to optimize the location of the zigzag cutouts and their respective tip masses to minimize the vibration of the plates P1 and P2 (Fig. 4). The optimization of P1 and P2 will be referred to as Case 1 and Case 2, respectively. The optimization parameters for both cases are the locations and the weight of the tip masses of the zigzag cutouts. The location of the zigzag is determined by (x, y) where x and

y are the coordinates of the lower-left side of the zigzag opening, and the origin is at the lower-left corner of the plate, as illustrated in Fig. 7. The optimization parameters are:
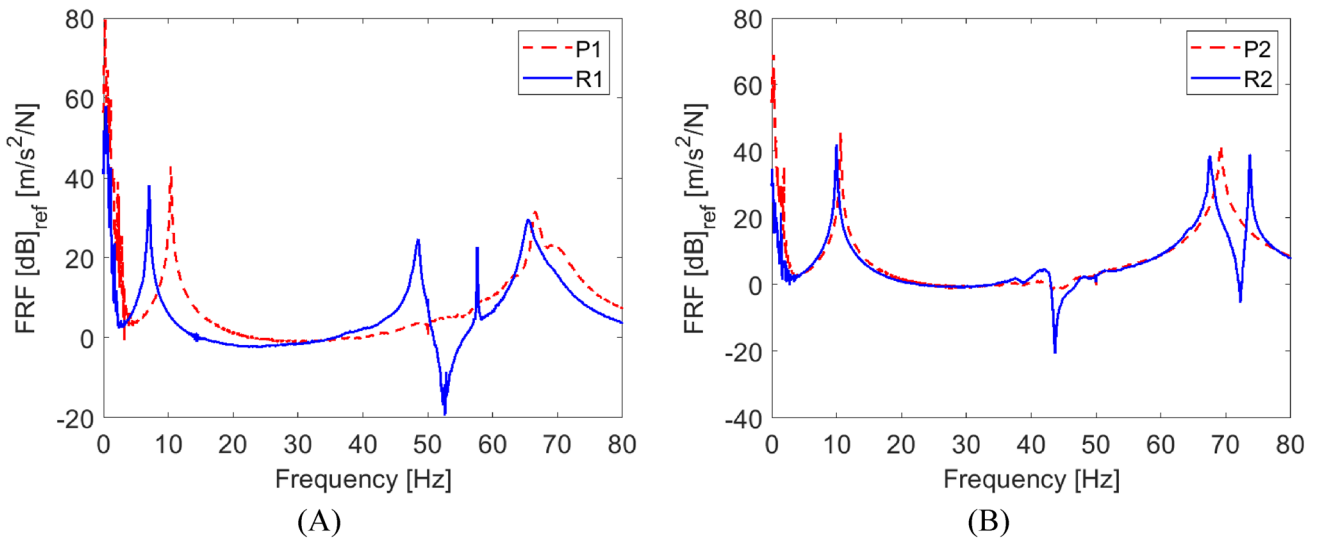
Fig. 6 Experimental frequency response function for Case1: **A** P1 and R1, Case 2: **B** P2 and R2 (defined in Table 1)
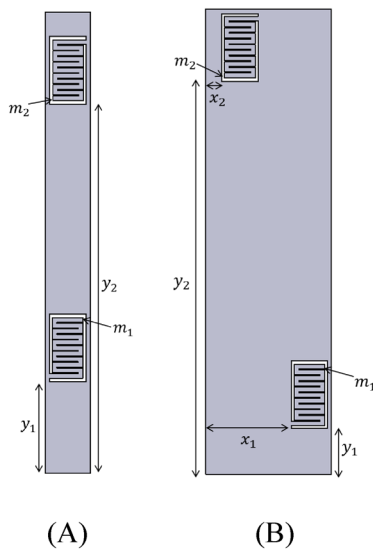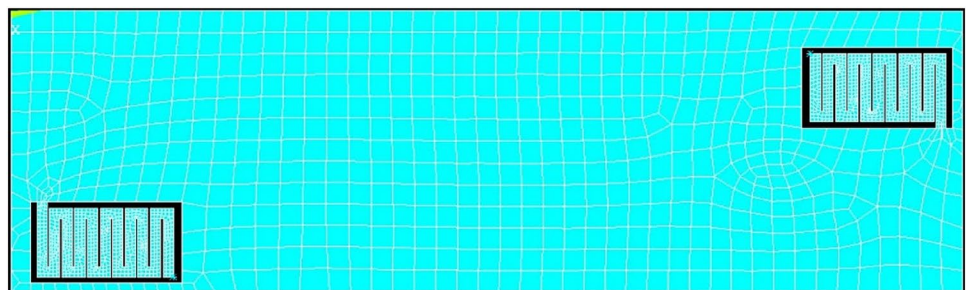

Fig. 7 Optimization parameters **A** Case 1 **B** Case 2

Fig. 8 FE model of a plate with zigzag cutouts with refined mesh at the zigzag beams

- y_1, m_1, y_2, m_2 for Case 1
- $x_1, y_1, m_1, x_2, y_2, m_2$ for Case 2

Numerical Modelling

Multiple finite element (FE) models representing the different plates in this section were developed in ANSYS® [22], as illustrated in Fig. 8. The FE simulations were used to obtain the frequency response function of the aluminum plates by running a modal analysis followed by a harmonic analysis over the 1–100 Hz frequency range. The model's response was computed in the frequency domain under harmonic excitation, mimicking the experimental setup described in the previous section. A base excitation is applied at the bottom of the plate, and the output is calculated at output location (*j*), illustrated in Fig. 3. This simulation aims to develop a reliable numerical model that can be used in the optimization process. The model was meshed with the SHELL281 element. SHELL 281 element has eight nodes
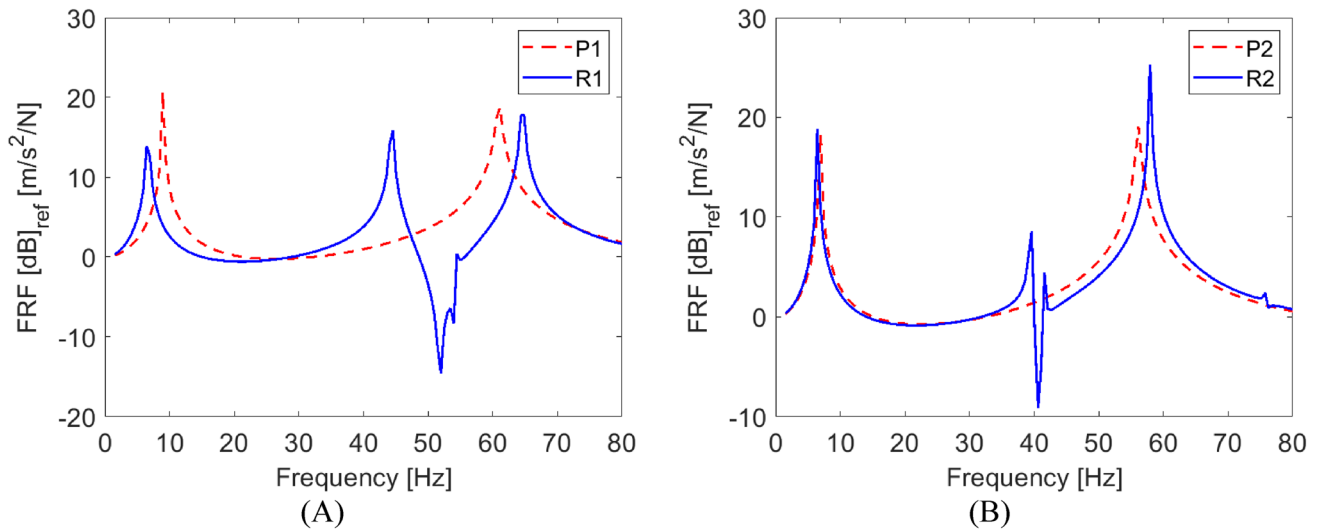
Fig. 9 Numerical FRFs for specimens for Case1: **A** plain plate P1 with random plate R1, Case 2: **B** plain plate P2 with random plate R2

with six degrees of freedom at each node (three translations and three rotations). A mesh convergence study was performed, and appropriate refinements at the zigzag cutouts were implemented. The linear elastic material model was assumed for the aluminum plate with an elastic modulus of 72 GPa, a Poisson ratio of 0.33, and a density of 2700 kg/m³.

The numerical FRFs of specimens P1, R1, P2, and R2 are shown in Fig. 9. The experimental FRFs of P1 and R1 are compared to their numerical counterparts in Fig. 10. There is good agreement between the experimental FRFs and the numerical FRFs. The numerical results obtained in this section provided confidence to proceed with optimizing the plate with zigzag cutouts. A MATLAB® code was then

written to generate an FE model (in ANSYS) of the plate from the variable set of parameters (position of the zigzag and the tip mass), while other parameters are constant such as the geometry of the plate and the material properties. The optimization parameters and codes are described in the following subsection.

Optimization Algorithm and Fitness Function

Genetic algorithms (GAs) use functions inspired by biological evolution and adaption. A GA uses the fitness function to search for the optimum solution from multiple points in parallel [23]. Therefore, this algorithm allows finding the
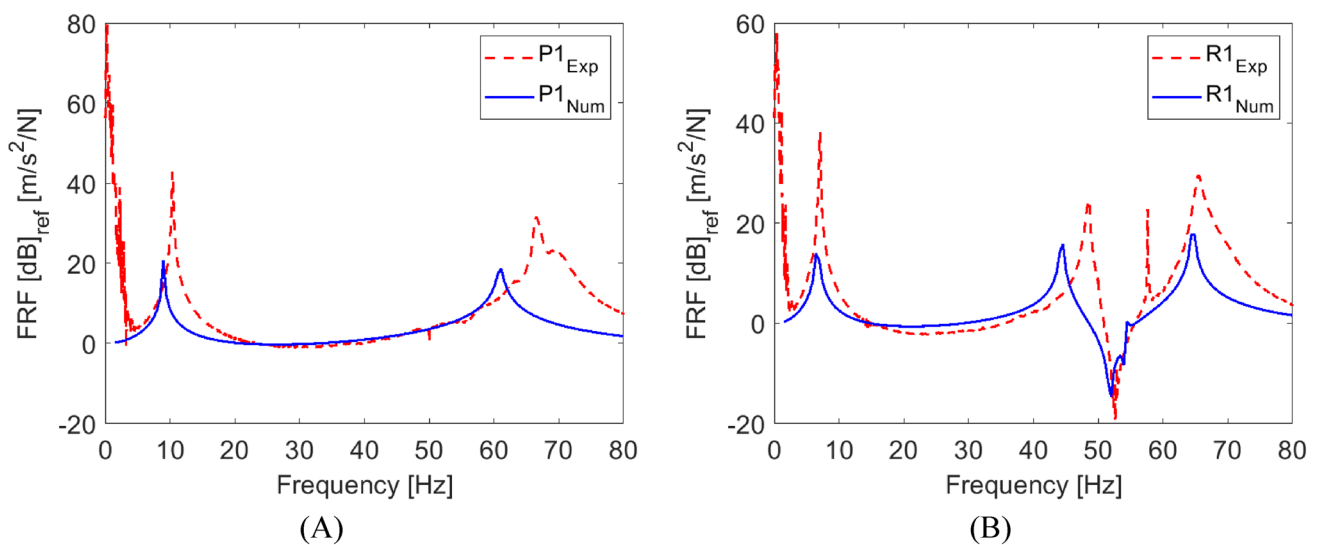

Fig. 10 Experimental vs. numerical FRFs of P1 and R1
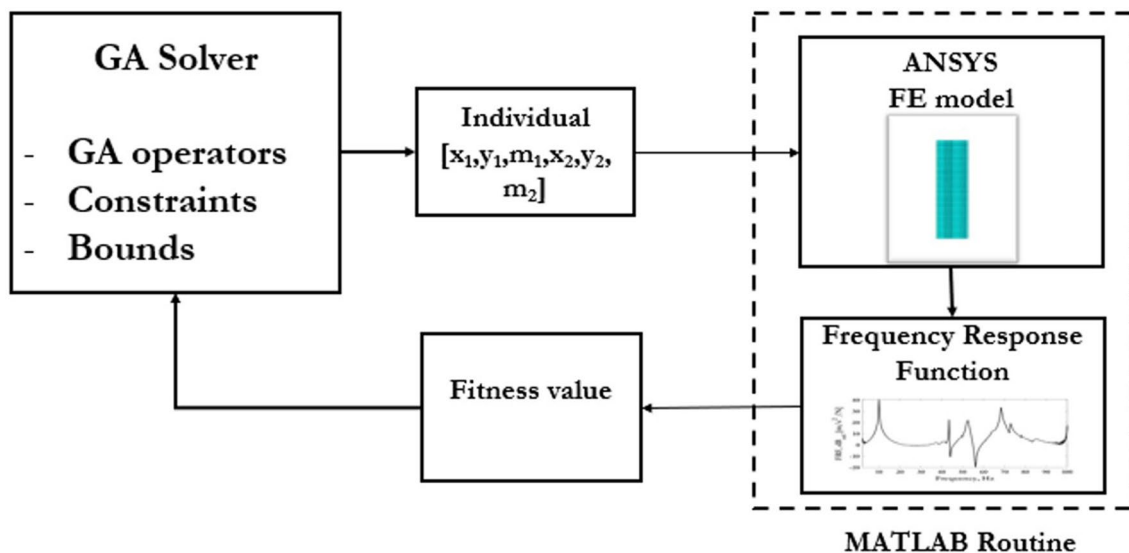
Fig. 11 The layout of the optimization process

global optima where conventional optimization methods risk being stuck in local optima where multiple local optima are expected. Moreover, GAs overrides the continuity and existence of derivatives problems [24].

In this study, GA has been performed to minimize vibration transmission in the two cases of thin aluminum plates for the 60–80 Hz frequency range. The fitness value of the proposed optimization is the root-mean-square (RMS) in the (60–80 Hz) range of the FRF of the specimen. The closer the RMS is to zero, the better the vibration attenuation performance of the specimen. A MATLAB routine was written to act as a fitness function of the optimization [25]. This routine generates a FE model of the plate with the zigzag cutouts in ANSYS®, conducts a modal analysis followed by a harmonic analysis in the range 1–100 Hz, and returns the FRF between the output and input acceleration within the desired frequency range. The fitness value is the RMS of the FRF in the 60–80 Hz frequency range. The population size selected for this optimization is 20. The optimization process is demonstrated in Fig. 11.

In this optimization, two linear constraints were imposed on the optimization routine. The first constraint ensures that the zigzag remains within the plate dimensions without being less than 2 mm away from its edges for laser cutting feasibility. The second constraint ensures that the two zigzag cutouts do not interlope with each other's and remain 2 mm away in both orthogonal directions. The tip masses have been limited to 20 g to ensure they remain on the zigzag's tip. These constraints are depicted in Eqs. (1) and (2) for Case 2.

$$
\begin{bmatrix} 0.002 \\ 0.002 \\ 0.002 \\ 0.002 \\ 0 \\ 0 \end{bmatrix} \leq \begin{bmatrix} x_1 \\ x_2 \\ y_1 \\ y_2 \\ m_1 \\ m_2 \end{bmatrix} \leq \begin{bmatrix} W - w_z - 0.002 \\ W - w_z - 0.002 \\ H - h_z - 0.002 \\ H - h_z - 0.002 \\ 20 \\ 20 \end{bmatrix} \tag{1}
$$

$$
\begin{bmatrix} |x_1 - x_2| \\ |y_1 - y_2| \end{bmatrix} \leq \begin{bmatrix} w_z + 0.002 \\ h_z + 0.002 \end{bmatrix}, \tag{2}
$$

where W is the total width of the plate, w_z is the width of the zigzag opening, H is the total height of the plate, h_z is the zigzag's opening height. These constraints ensure that the optimal specimen can be manufactured using the available methods and further demonstrate the practicality of the proposed approach. Similar equations can be written for Case 1 with $x_1 = x_2 = 5$ mm.

Optimization Algorithm and Fitness Function

Case 1

The first GA optimization was conducted for P1 to find the optimal locations and tip masses of the zigzag cutouts that minimize the plate's vibration within the 60–80 Hz frequency range. The GA took 27 generations to converge to the optimal specimen illustrated in Fig. 12 and detailed in Table 3. The optimal specimen, O1, is a plate with two

Fig. 12 Optimal specimen O1:
A contour plot of the FE model,
B fabricated specimen
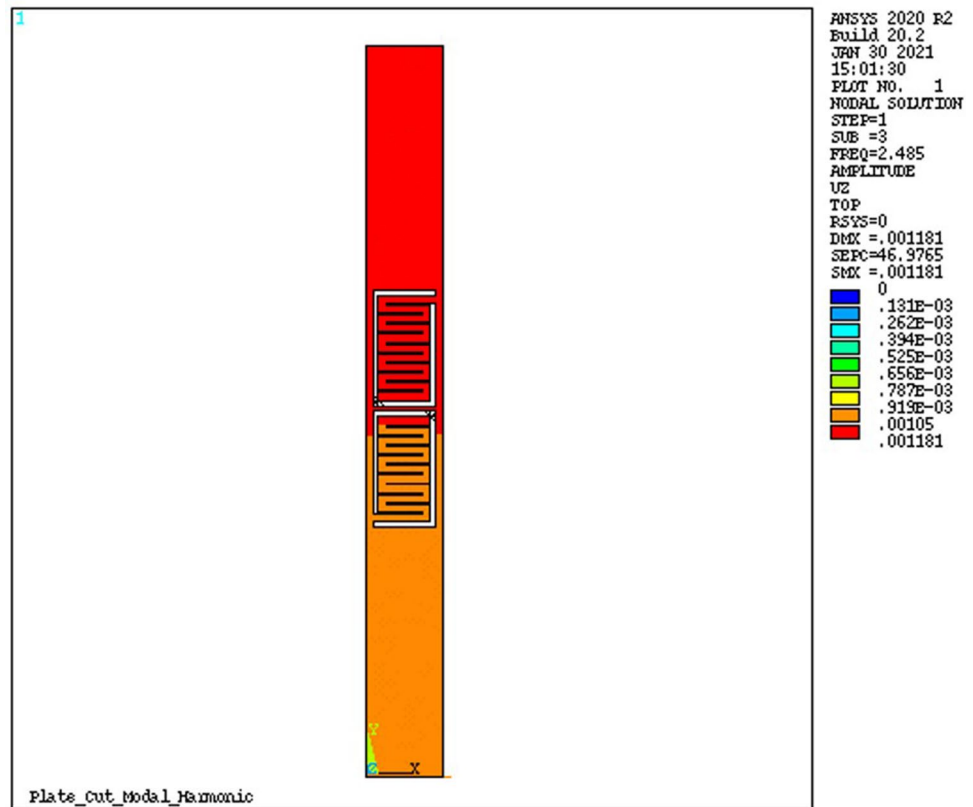
zigzags around its middle section with 3.9 g and 13.4 g tip masses.

The optimal specimen O1 was manufactured and tested in the experimental conditions described earlier. Figure 13 shows the numerical and experimental FRFs of the optimal specimen O1 and the plain plate P1. There is a clear low transmission zone in the 60–80 Hz range, replacing the original resonance zone in the corresponding plain plate. It is worth mentioning that the numerical RMS values in that frequency range are 17, 10.8, and 0.3 mm/s^2/N, for P1, R1, and O1, respectively. Thus, the presence of the zigzag cutouts has successfully suppressed the vibration of the plate in the target frequency range. The optimization of the FE model using GA yielded an optimal specimen with satisfactory experimental FRF; thus, the optimization of Case 1 is reliable.

Table 3 First optimization results

Optimization parameters	Optimal values
y_1	158.8 mm
m_1	3.9 g
y_2	231.9 mm
m_2	13.4 g

Case 2

The second GA optimization was conducted for P2 to find the optimal locations and tip masses of the zigzag cutouts that minimize the plate's vibration within the 60–80 Hz frequency range. The GA took 36 generations to converge to the optimal specimen, O2, illustrated in Fig. 14 and detailed in Table 4. The optimal specimen is a plate with two zigzags with 4 g and 7.3 g tip masses.

The optimal specimen O_2 was manufactured and tested in the experimental conditions described earlier. Figure 15 shows the numerical and experimental FRFs of the optimal specimen O2 and the plain plate P2. Observing the 60–80 Hz range in Fig. 15, two narrow low transmission zones appear around 60 and 70 Hz, replacing the high transmission zone in the corresponding plain plate. The resulting numerical RMS values are 14.8, 19.7, and 6.3 mm/s^2/N, for P2, R2, and O2, respectively. Again, in this case, the zigzag cutouts in the optimal configuration minimize the vibration of the plate in the target frequency range. Thus, the optimization process of P2 resulted in an optimal specimen O2 with satisfactory experimental FRF.
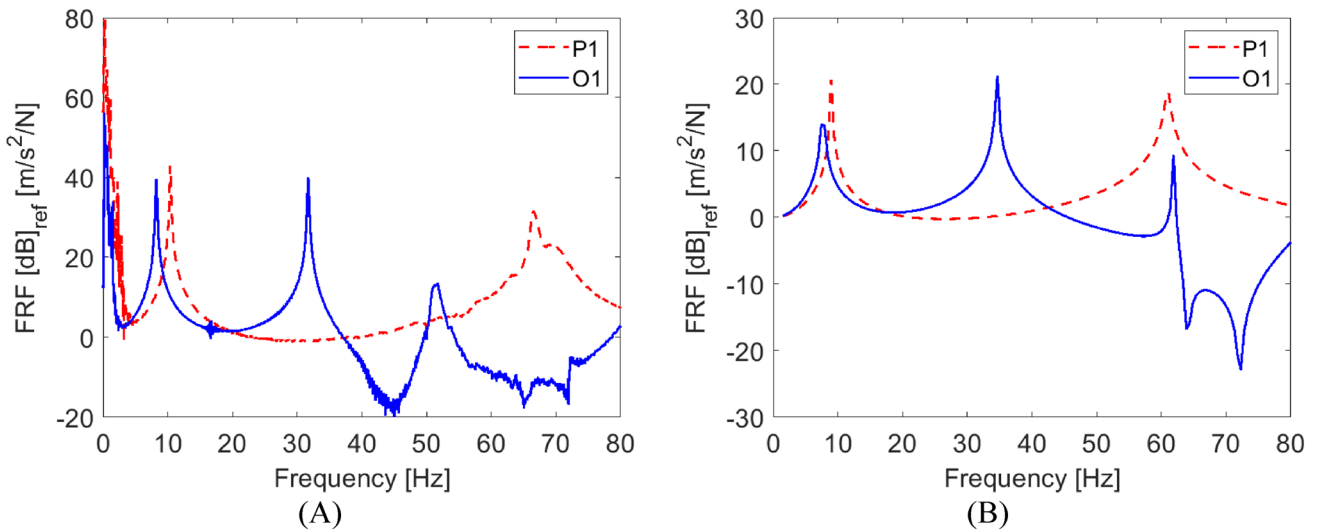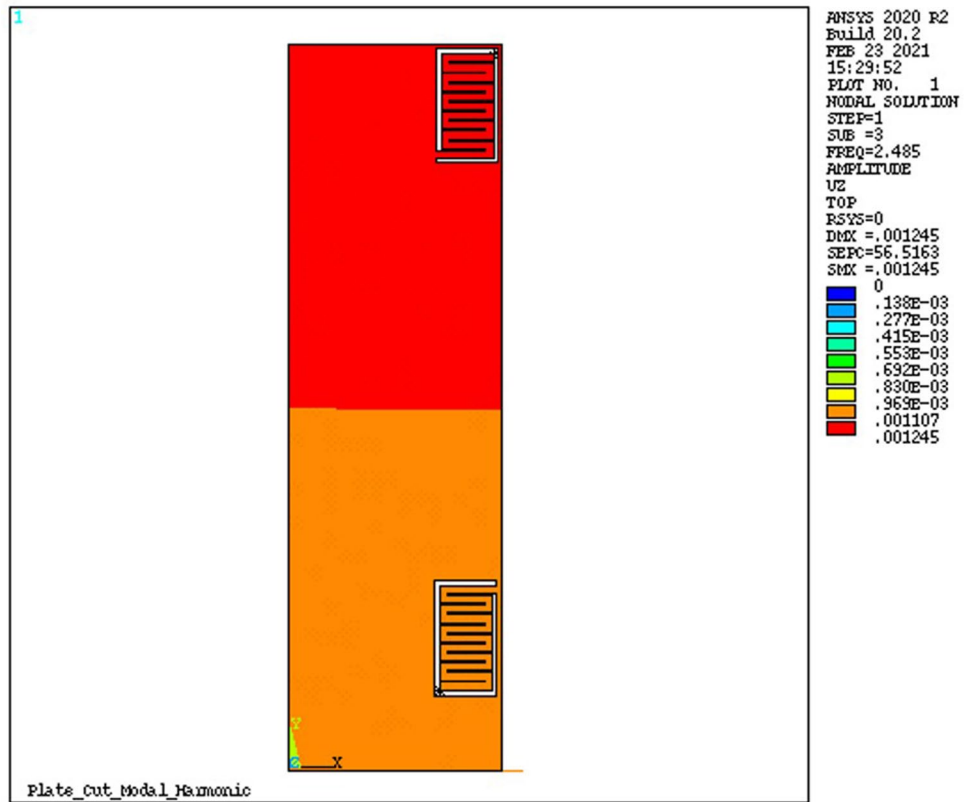
Fig. 13 Comparison between the FRFs of the optimal specimen O1 and the corresponding plain plate P1 **A** experimental **B** numerical

Fig. 14 Optimal specimen O2:
A contour plot of the FE model,
B fabricated specimen

Conclusion

For two-dimensional mechanical metastructures, one of the most common vibration attenuation mechanisms is the use of local resonators, where the resonant components in a host structure interact with the long wavelength of the traveling wave leading to wave transmission restrictions. In this study,

zigzag beams are cut out in an aluminum plate to generate targeted low transmission zones with minimum structural intervention. Plain plates and plates with randomly located zigzag cutouts were tested experimentally using a shaker, and vibration was measured using accelerometers. Comparing the frequency response functions (FRFs) of the plates with randomly located zigzag cutouts with the FRFs of the

Table 4 Second optimization results

Optimization parameters	Optimal values
x_1	93 mm
y_1	385 mm
m_1	4 g
x_2	93 mm
y_2	47.2 mm
m_2	7.3 g

corresponding plain plates shows that two zigzag cutouts can generate a low transmission zone. The plates were modeled using the finite element (FE) method to optimize the location of the zigzag cutouts and their tip masses. The FE models were coupled with a genetic algorithm (GA) to find the optimal zigzag cutout configuration. The fitness function for the GA was the root-mean-square (RMS) of the plate's vibration at its free end. Physical and practical constraints were enforced on the optimization problem to ensure that the obtained solution is manufacturable. Two host structures were considered. In the first case, a plate with two aligned zigzag cutouts was considered where the GA had to find the optimal locations of the zigzag cutouts and the optimal tip masses. This optimization problem has four parameters. In the second case, a plate with two non-aligned zigzag cutouts was considered where the GA had to find the optimal linear and transverse location of each zigzag cutout and the optimal tip mass for each zigzag. This optimization problem was more challenging and involved six parameters. The optimal plates were manufactured and tested experimentally. Numerical and experimental results demonstrate that the zigzag cutouts introduced a low transmission zone in the targeted frequency range. The comparison between the experimental FRFs of the optimal specimens shows that the optimization

has been reliable and can be used to tune the plate to match its structural dynamic service needs. Although the developed approach was demonstrated for the case of a plate, the methodology is general and can be extended to suppress the vibration of other host structures.

References

1. Kaina N, Fink M, Lerosey G (2013) Composite media mixing bragg and local resonances for highly attenuating and broad band-gaps. Sci Rep 3240
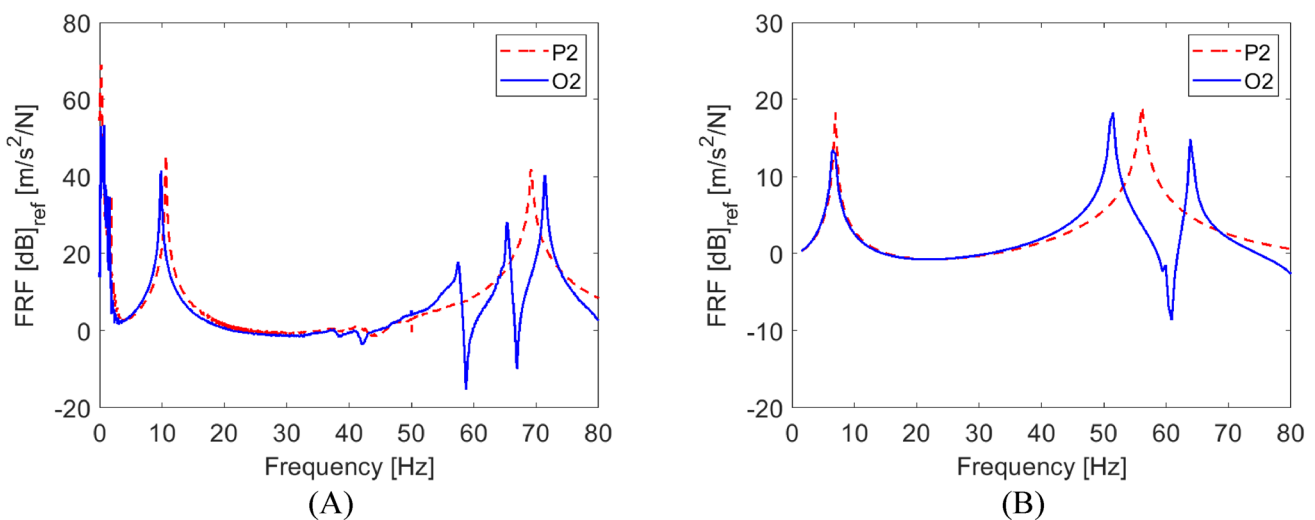

Fig. 15 Comparison between the FRFs of the optimal specimen O2 and the corresponding plain plate P2 **A** experimental **B** numerical

2. Al Ba'Ba'A H, Nouh M (2017) An investigation of vibrational power flow in one-dimensional dissipative phononic structures. J Vib Acoust Trans ASME 021003:10

3. Meng H, Chronopoulos D, Bailey N, Wang L (2020) Investigation of 2D rainbow metamaterials for broadband vibration attenuation. Materials 13(22):1–9

4. Nouh M, Aldraihem O, Baz A (2014) Vibration characteristics of metamaterial beams with periodic local resonances. J Vib Acoust Trans ASME 061012:12

5. Elmadih W, Chronopoulos D, Syam WP, Maskery I, Meng H, Leach RK (2019) Three-dimensional resonating metamaterials for low-frequency vibration attenuation. Sci Rep 9(1):1–8

6. Krushynska AO, Miniaci M, Kouznetsova VG, Geers MGD (2017) Multilayered inclusions in locally resonant metamaterials: two-dimensional versus three-dimensional modeling. J Vib Acoust Trans ASME 024501:4

7. Krushynska AO, Miniaci M, Bosia F, Pugno NM (2017) Coupling local resonance with Bragg band gaps in single-phase mechanical metamaterials. Extreme Mech Lett 12:30–36

8. Liu Z, Zhang X, Mao Y, Zhu YY, Yang Z, Chan CT, Sheng P (2000) Locally resonant sonic materials. Science (1979) 289(5485):1734–1736

9. Pai PF (2010) Metamaterial-based broadband elastic wave absorber. J Intell Mater Syst Struct 21(5):517–528

10. Sun H, Du X, Pai PF (2010) Theory of metamaterial beams for broadband vibration absorption. J Intell Mater Syst Struct 21(11):1085–1101

11. Pai PF, Peng H, Jiang S (2014) Acoustic metamaterial beams based on multi-frequency vibration absorbers. Int J Mech Sci 79:195–205

12. Guo Z, Sheng M, Pan J (2017) Flexural wave attenuation in a sandwich beam with viscoelastic periodic cores. J Sound Vib 400:227–247

13. Bailey T, Ubbard JE (1985) Distributed piezoelectric-polymer active vibration control of a cantilever beam. J Guid Control Dyn 8(5):605–611

14. Chen B, Shiryayev O, Vahdati N, El-Sinawi A (2019) Validation of a modeling tool for in-plane longitudinal resonators with zigzag topology. Int J Appl Mech 11(2):1950013

15. Ji JC (2012) Application of a weakly nonlinear absorber to suppress the resonant vibrations of a forced nonlinear oscillator. J Vib Acoust Trans ASME 044502:6

16. Hobeck JD, Inman DJ (2015) Magnetoelastic metastructures for passive broadband vibration suppression. Active Passive Smart Struct Integr Syst 9431:943119

17. Essink BC, Hobeck JD, Owen RB, Inman DJ (2015) Magnetoelastic energy harvester for structural health monitoring applications. Active Passive Smart Struct Integr Syst 9431:943123

18. Karami MA, Inman DJ (2011) Analytical modeling and experimental verification of the vibrations of the zigzag microstructure for energy harvesting. J Vib Acoust Trans ASME 011002:10

19. Abdeljaber O, Avci O, Kiranyaz S, Inman DJ (2017) Optimization of linear zigzag insert metastructures for low-frequency vibration attenuation using genetic algorithms. Mech Syst Signal Process 84:625–641

20. Lu Z, Wang Z, Zhou Y, Lu X (2018) Nonlinear dissipative devices in structural vibration control: a review. J Sound Vib 423:18–49

21. Zhou CW, Lainé JP, Ichchou MN, Zine AM (2015) Wave finite element method based on reduced model for one-dimensional periodic structures. Int J Appl Mech 7(2):15500018

22. ANSYS Inc. (2009) Ansys® Academic Research Mechanical, Release 17.0, Help System, Element Library. ANSYS Inc.

23. Mathias J-D, Balandraud X, Grediac M (2006) Applying a genetic algorithm to the optimization of composite patches. Comput Struct 84(12):823–834

24. Heiss-Czedik D (1997) An Introduction to Genetic Algorithms. In Artificial Life 3(1):63–65. https://doi.org/10.1162/artl.1997.3.1.63

25. Ghachi RF, Alnahhal WI, Abdeljaber O, Renno J, Tahidul Haque ABM, Shim J, Aref A (2020) Optimization of viscoelastic metamaterials for vibration attenuation properties. Int J Appl Mech 12(10):2050116